

Three-Dimensional Mathematical Modeling of Fluid Flow in Slab Tundishes and Its Verification with Water Model Experiments

J.-L. Yeh, W.-S. Hwang, and C.-L. Chou

A three-dimensional mathematical model has been developed based on the incorporation of a computational fluid dynamics technique, called SOLA-SURF, and the K-ε turbulence model. Numerical solutions of the three-dimensional turbulent Navier-Stokes equations and the K and ε equations together with the free surface treatment are presented to study the turbulent flow behavior of molten steel in tundishes. Computed results describing the three-dimensional flow field, particle path lines, residence time distribution curve during steady-state operation are presented. The values of t_{min}, t_{peak}, and t_{mean} derived from the residence time distribution curve are used to evaluate the effects of using various combinations of flow control devices such as dams, weirs, and dams with a hole in the flow field. The computed results were compared with the experimental data obtained from a full-scale plexiglas/water model of tundish. The comparisons exhibited good consistency.

1. Introduction

QUALITY concerns in continuous casting processes have become more and more crucial with progressively increasing machine throughputs and larger product dimensions. As a result, steel cleanliness and strict composition control are now of primary concern for steelmakers. A tundish is an intermediate vessel that taps the molten steel from the ladle and distributes it to the casting mold. However, to produce cleaner steel, the tundish is also used, in addition to its conventional role, as a vessel/reactor for inclusion removal.

To remove inclusions from the molten steel, the particles have to float to the top and become trapped by the slag layer. From the standpoint of tundish design and operation, the residence time of the molten steel must be prolonged, and the path line of the inclusion particle should favor its entrapment by the surface slag. Therefore, the velocity distribution of molten steel within the tundish is very influential on the removal of inclusion particles. It is known that, by properly inserting flow control devices such as dam and/or weir, the flow of molten steel can be controlled, and thus most of the inclusions can be removed. Therefore, it is then desirable to understand how designs in the tundish can affect the flow characteristics of the molten steel and the particles to obtain proper design of the tundishes.

Basically, there are three ways to investigate these correlations. First, experiments can be conducted in the actual tundish-molten steel system. The results are direct and supposedly most accurate. However, it is very expensive and extremely difficult to visualize what really happened.

The second approach is to use a physical model. The most common method of tundish study is to use acrylic to construct

J.-L. Yeh and **W.-S. Hwang**, Graduate School of Mineral, Metallurgy and Materials Science, National Cheng Kung University, Tainan, Taiwan, R.O.C.; and **C.-L. Chou**, Steel & Aluminum Research and Development Department, China Steel Corporation, Kaohsiung, Taiwan, R.O.C.

Symbols	
C	Concentration of tracer, kg/m^3
C_1, C_2, C_3, C_d	Empirical constants in the K-ε turbulence model
d_i	Width of the inlet nozzle, m
D_e	Effective diffusivity, m^2/sec
D_m	Molecular diffusivity, m^2/sec
g_i	Gravitational constant in vector notation, i = 1, 2, 3 corresponding to x, y, z directions, m/sec^2
h	Height of the liquid, m
K	Turbulence kinetic energy, m^2/sec^2
K_i	K value at the inlet nozzle, m^2/sec^2
$n, n+1$	Old time level and new time level, respectively
P	Pressure, kg/m · sec^2
R_p	Radius of the inclusion particle, m
t	Time, sec
t_{mean}	Mean residence time, min
t_{min}	Minimum residence time, sec
t_{peak}	Peak residence time, min
u, v, w	Mean velocity components in x, y, z directions, m/sec
u_i, u_j	Mean velocity in vector notation, i, j = 1, 2, 3 corresponding to x, y, z directions, m/sec
U_i	Normal inlet velocity, m/sec
V_t	Rising velocity, m/sec
x, y, z	Lateral (length), vertical, and width directed coordinates with respect to a rectangular tundish
x_i, x_j	Coordinate axes in vector notation, i, j = 1, 2, 3 corresponding to x, y, z directions, m
δt	Time step, sec
ε	Dissipation rate of turbulence energy, m^2/sec^3
ε_i	ε value at the inlet nozzle, m^2/sec^3
μ_m	Molecular viscosity, m^2/sec
ν_e	Effective kinematic viscosity, m^2/sec
ν_m	Molecular kinematic viscosity, m^2/sec
ν_t	Turbulent kinematic viscosity, m^2/sec
ρ_l	Density of the liquid, kg/m^3
ρ_p	Density of the inclusion particle, kg/m^3
σ_k, σ_e	Schmidt numbers for K and ε

the vessel and use water to replace molten steel.[1] The primary advantage of the acrylic/water model is that it is relatively easy to observe and measure the liquid flow in the vessel. However, according to the similarity theory, the flow behavior of the water is similar to that of the molten steel in the tundish, if and only if the Reynolds numbers and Froude numbers of both systems are equal. Because the kinematic viscosity of water is very close to that of molten steel, the water model must be a full-scale model to accurately simulate the flow behavior of the molten steel in the tundish. A full-scale acrylic/water model is also rather expensive and not very flexible if varying designs and operation conditions are to be studied.

The third approach is to use a mathematical modeling technique.[2-6] For tundish study, it first uses a set of partial differential equations and appropriate boundary conditions to mathematically represent the flow phenomena of molten steel in the tundish. Then, the partial differential equations are formulated, using a numerical technique, into a set of algebraic expressions. Finally, a computer program is developed based on these algebraic expressions and boundary conditions. When the program is executed, it is provided with a set of input data that represents the design and operation conditions. The computed results are then interpreted and much detailed information, such as the flow field, path line of the inclusion, and residence times of inclusions, can be obtained. One of the major advantages of the mathematical model is that it is extremely flexible.

For the above-mentioned reasons, it was the goal of this study to develop an efficient numerical tool to elucidate the flow phenomena of molten steel and inclusion particles in the tundish. Reviewing the literature, it was noted that a number of similar efforts had been made. DebRoy and Sychterz[2] developed a two-dimensional mathematical model to evaluate tundish design by calculating the flow field and particle path lines.

Considerable effort has also been made to develop three-dimensional mathematical models for turbulent flow in the tundishes. Szekely *et al.*[3] used a commercial package, called Phoenix, to predict the flow field, turbulence kinetic energy isopleths, and residence time distribution (RTD) curves in the tundishes. Tacke and Ludwig[4] also developed a model to compute the flow field and to evaluate the percentage of removed particles by the particle concentration field. They also investigated the influence of increased tundish width and height and of dams and weirs on the rate of inclusion separation.

Lai *et al.*,[5] and He and Sahai[6] also used mathematical models to study the above flow characteristics in tundishes, in which no flow control devices were used. However, in these studies, the free surface of molten steel in the tundish was assumed to be flat and constant. Also, the effects of flow control devices on certain flow characteristic values such as t_{min}, t_{peak}, and t_{mean} of residence time distribution curves were not evaluated quantitatively. It is also known that a water model must be full-scale to accurately simulate the flow behavior of the molten steel in the tundish. The previous studies either have not compared their calculated results with experiments or have compared the results with water models of reduced scale.

A two-dimensional mathematical model had been developed by the authors[7] based on a computational fluid dynamics technique, called SOLA-SURF[8] to analyze the flow behavior of the fluid and to quantitatively evaluate the effect of flow control devices on the flow characteristics such as t_{min}, t_{peak}, and t_{mean} of the residence time distribution curves in the tundishes. It can also calculate the configuration of free space during steady-state operation, the variations of free surface during the beginning and ending of the casting operation, and during ladle interchange. Undoubtedly, to model the flow behavior in the tundish meaningfully, a three-dimensional model must be developed. The two-dimensional model developed earlier provided a solid foundation for the development of a three-dimensional model.

In this study, a three-dimensional mathematical model was developed based on the two-dimensional model previously undertaken to investigate the flow phenomena of molten steel in tundishes of varying design and operating conditions. The model is again based on the SOLA-SURF technique. Moreover, it is a well-known fact that the flow of molten steel in a tundish is basically a turbulent flow phenomenon. In an engineering approach, the extra momentum transfer due to turbulence is usually considered to be due to turbulence viscosity. Unlike material viscosity, the turbulence viscosity is a system property and varies with time and position in the tundish. Turbulence viscosity is generally estimated with a turbulence model. In the previous two-dimensional model, a very rough turbulence model (namely Prandtl's mixing length hypothesis) was used.[9]

In the present model, a more accurate turbulence model (namely the K-ε two equation model) was used to estimate the turbulence viscosity.[10] Also, to be used as a design tool, a mathematical model first needs to be verified for its accuracy and reliability. A full-scale water/plexiglas model was used in this study to experimentally observe the flow phenomena and measure the flow properties. Particularly, residence time distribution curves were measured and certain characteristic values, such as t_{min}, t_{peak}, and t_{mean}, were obtained. These parameters can be used to evaluate the efficiency of inclusion removal in the tundish and thus are the appropriate parameters to be compared with the mathematical model. Because the model was verified for its reliability, it was then used as a design tool to evaluate the effect of tundish design, such as the placement of

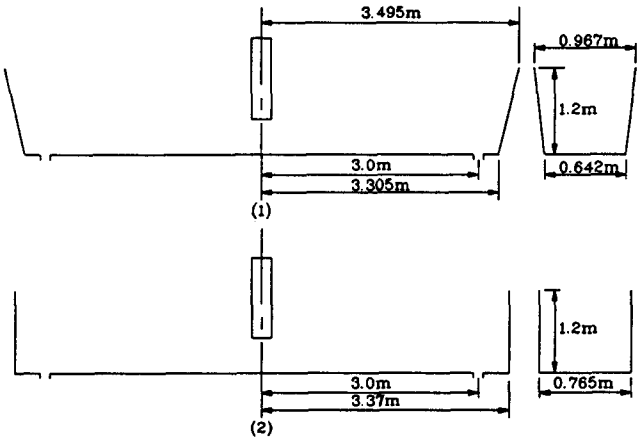

Fig. 1 Dimensions of an actual tundish (1). Dimensions of the tundish analyzed in the mathematical model (2).

Table 1 Constants Used in the K-ε Turbulence Model

C_1	C_2	C_3	σ_k	σ_e
1.44	1.92	0.09	1.0	1.3

different flow control devices. The flow control devices include weir, dam, dam with a hole, and combinations thereof.

2. Mathematical Model

2.1 *Assumptions*

To conduct an analysis of fluid flow phenomena in the tundish of a continuous casting process, certain assumptions were made to ease the complexity of the task. First, the fluid flow was assumed to be isothermal. Second, the actual tundish had a tilted wall, as shown in Fig. 1 (part 1). In this study, the tundish was assumed to be rectangular, as shown in Fig. 1 (part 2). Furthermore, it was assumed that the existence of the surface slag layer does not significantly influence the fluid flow of the molten steel. Also, when calculating the trajectories of the inclusion particles, the particles were assumed to be so small that they would flow along with the molten steel and would not affect the flow of the molten steel.

2.2 *Governing Equations*

For the three-dimensional turbulent flow calculations, the governing equations used in the Cartesian vector notation are as follows:

Equation of continuity:

$$\frac{\partial u_i}{\partial x_i} = 0 \qquad [1]$$

Equations of momentum:

$$\frac{\partial u_i}{\partial t} + \frac{\partial u_i u_j}{\partial x_j} = -\frac{1}{\rho_l}\frac{\partial P}{\partial x_i} + \frac{\partial}{\partial x_j}\left[\nu_e\left(\frac{\partial u_i}{\partial x_j} + \frac{\partial u_j}{\partial x_i}\right)\right] + g_i \qquad [2]$$

where

$$\nu_e = \nu_m + \nu_t \qquad [3]$$

Equations 1 and 2 are also called Navier-Stokes equations. As shown in the above equations, the effective kinematic viscosity, ν_e, is used to represent the combined effects of molecular and turbulence viscosities.

2.3 *Turbulence Model*

In this study, the K-ε turbulence model[10] was used to estimate the turbulence viscosity. Here, turbulence is expressed in terms of the turbulence kinetic energy, K, and its rate of dissipation, ε. The relation between ν_t and the two turbulence characteristics is as follows:

$$\nu_t = \frac{C_3 K^2}{\varepsilon} \qquad [4]$$

These two characteristics of turbulence are again described by two differential equations, which can be derived from the Navier-Stokes equations and the basic definition of turbulence. The governing equations for K and ε are as follows.

Equation for turbulence kinetic energy:

$$\frac{\partial K}{\partial t} + \frac{\partial u_i K}{\partial x_i} = \frac{\partial}{\partial x_i}\left[\frac{\nu_t}{\sigma_k}\frac{\partial K}{\partial x_i}\right] + \nu_t \frac{\partial u_j}{\partial x_i}\left[\frac{\partial u_i}{\partial x_j} + \frac{\partial u_j}{\partial x_i}\right] - \varepsilon \qquad [5]$$

Equation for dissipation rate of turbulence kinetic energy:

$$\frac{\partial \varepsilon}{\partial t} + \frac{\partial u_i \varepsilon}{\partial x_i} = \frac{\partial}{\partial x_i}\left[\frac{\nu_t}{\sigma_e}\frac{\partial \varepsilon}{\partial x_i}\right] + \frac{C_1 \varepsilon \nu_t}{K}\frac{\partial u_j}{\partial x_i}\left[\frac{\partial u_i}{\partial x_j} + \frac{\partial u_j}{\partial x_i}\right] - \frac{C_2 \varepsilon^2}{K} \qquad [6]$$

The five empirical constants appearing in Eq 4 to 6 were adopted based on the suggestions by Launder and Spalding,[10] and their values are shown in Table 1.

2.4 *Method of Monitoring Variations in the Free Surface*

In SOLA-SURF, a height function method is used to represent the free surface configuration and monitor of its evolution. The method defines a height function value, which is the height of the free surface to a reference plane as a function of position along the reference plane (for example, $h = f(x,z)$). The time evolution of the height function is governed by a kinematic equation expressing the fact that the surface must move with the fluid, which is shown as follows:

$$\frac{\partial h}{\partial t} + u\frac{\partial h}{\partial x} + w\frac{\partial h}{\partial z} = v \qquad [7]$$

2.5 *Movement of Inclusion Particles*

The nonmetallic inclusion is lighter than the molten steel. It, therefore, will float due to the buoyancy force acting on the particle. Assuming that inclusion particles are spherical and that the collision of particles will not result in division or combination of the particles, the rising velocities of the inclusion particles can be calculated with the following equation, which was derived from the Stokes law:[12]

$$V_t = \frac{2R_p^2(\rho_l - \rho_p)g}{9\mu_m} \qquad [8]$$

As the steady-state velocity field is obtained, five particles (10 μm in size) are released from the inlet nozzle. The particle path line simulates how the inclusions will flow along with the molten steel. The size of the particles, R_p, can easily be changed to evaluate the removal efficiency for inclusions of different sizes. The positions of the particles can be computed with the following equations:[2]

$$x^{n+1} = x^n + \delta t \cdot u_{x,y,z} \quad [9]$$

$$y^{n+1} = y^n + \delta t \cdot (v_{x,y,z} + V_t) \quad [10]$$

$$z^{n+1} = z^n + \delta t \cdot w_{x,y,z} \quad [11]$$

The new positions of the particles can be repeatedly calculated as time proceeds according to the above equations until the particles exit from the tundish or float to the top.

2.6 *Residence Time Distribution Curve*

To calculate the residence time distribution curve of the molten steel and compare it to a curve obtained from the water model, a pulse of tracer was introduced into the melt through the inlet and allowed to flow with the melt. By monitoring the change in tracer concentration of the melt at the outlet, the residence time distribution curve was obtained. The transport of the tracer and the variation in tracer concentration is governed by the mass transport equation as follows:

$$\frac{\partial C}{\partial t} + \frac{\partial u_i C}{\partial x_i} = \frac{\partial}{\partial x_i}\left[D_e \frac{\partial C}{\partial x_i}\right] \quad [12]$$

where C represents the concentration of the tracer, and D_e is the effective mass diffusion coefficient, which depends on the flow field in a manner similar to the turbulence viscosity. In this study, D_e was assumed to relate to the effective kinematic viscosity, ν_e, in the following manner:

$$\frac{\nu_e}{\nu_m} \approx \frac{D_e}{D_m} \quad [13]$$

When the relationship between tracer concentration and time—namely the residence time distribution curve—is known, valuable information can then be obtained. The first observation of tracer at the outlet nozzle after an impulse of tracer has been injected into the tundish from the inlet nozzle is called the minimum residence time, or t_{min}. The time at which concentration reaches a maximum in the residence time distribution curve is called the peak residence time, or t_{peak}. The extent of plug flow is proportional to t_{peak}, and the size of the dead zone decreases with increasing plug flow. Naturally, a smaller dead zone is favorable. Also, the mean residence time, t_{mean}, is defined and estimated according to the following equation:

$$t_{mean} = \frac{\int_0^\infty t \cdot C \, dt}{\int_0^\infty C \, dt} \quad [14]$$

A larger value for t_{mean} indicates that the residence time of the molten steel is, on average, longer, which favors removal of the inclusion particles.

2.7 *Boundary Conditions*

In computational fluid dynamics, boundary conditions at the solid walls are treated in two ways. One is the free-slip treatment the other is the no-slip treatment. In this study, at the tundish wall, including dams, weirs, and the side wall of the ladle nozzle, the velocity components (u, v, and w) and the turbulence transport properties (K and ε) were imposed with no-slip wall boundary conditions. For velocity components normal to the wall, they were set to zero. For other flow quantities, zero fluxes were imposed. At the planes of symmetry, the normal velocity components and the normal gradients of all other variables were set to zero. At the inlet, tangential velocity was set to zero, whereas normal velocity was prescribed according to the inflow rate. The values of K and ε at the nozzle inlet were assumed to have the following relations:[10]

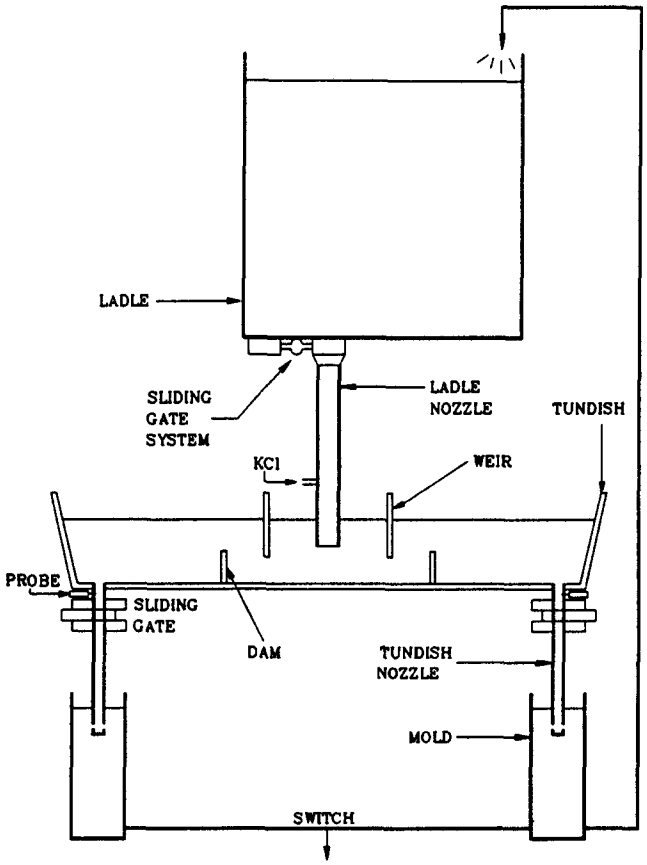

Fig. 2 Schematic diagram of the plexiglas/water model used in this study.

$$K_i = 0.01\, U_i^2 \quad [15]$$

$$\varepsilon_i = C_d \cdot K_i^{1.5} / (d_i / 2) \quad [16]$$

In this study, C_d is assumed to be unity.

The boundary conditions required for the solution of Eq 12 must satisfy the physical constraints that all of the bounding surfaces are impervious to the tracer. Mathematically, this corresponds to zero flux at all of the bounding surfaces.

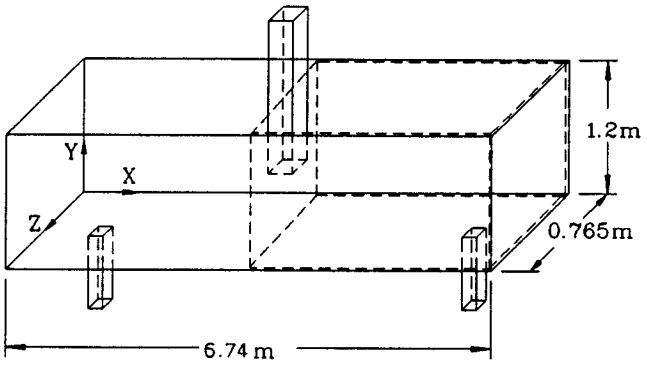

Fig. 3 Diagram of tundish to be modeled mathematically.

3. Physical Model

A full-scale water/plexiglas model of a typical slab tundish was used in this study to experimentally observe the flow phenomena in the tundish and measure the residence time distribution curves. A full-scale model must be used, because the similarity criteria require that the Reynolds number and Froude number be equal between the physical model and the real tundish. A schematic diagram of the water model used is shown in Fig. 2 and the dimensions of the tundish are shown in Fig. 1 (part 1). This full-scale water model is a transparent acrylic representation of an actual slab tundish used at the China Steel Corp. Water was filled to a height of 0.9 m, and its level was maintained with a casting speed of 1.2 m/min. A water stream poured from the ladle to the tundish, in which the nozzle was submerged about 0.3 m below the free surface of the water to prevent entrainment of air. The system could recirculate the water, and in case of dye injection, water could be by-passed to drain.

After steady-flow conditions were attained, a measured amount of solution of known concentration was injected into the ladle/tundish stream within the time of a pulse. Potassium chloride salt was added as the solute in the solution and was used as the tracer for the residence time distribution measurements. The concentration of the potassium chloride in the stream that reached the exit was monitored by an on-line conductivity instrument. The conductivity signal was transferred to a digital signal by an analog-digital (AD) converter, and the digital data along with the corresponding time were recorded on a personal computer. The experiment was continued until most of the solute left the tundish. The residence time distribution curve could then be obtained.

It should be noted that the water model experiment is very time-consuming and that the flow field and residence time distribution curve would be affected by different flow control devices. Therefore, only limited tundish designs were used in this study. The various designs include those with (1) no flow control devices, (2) a weir-dam combination, (3) a dam-weir-dam combination, and (4) a dam-weir-dam with a hole combination. The results are discussed in the following sections.

Table 2 System Parameters for the Various Tundish Designs Used in the Calculations

	Test case			
Parameter, m	1	2(a)	3(b)	4(c)
Position of weir	...	0.855	0.855	0.855
Height between tundish bottom and weir	...	0.12	0.12	0.24
Thickness of weir	...	0.09	0.09	0.09
Position of dam			0.405	0.405
	...	1.665	1.665	1.665
Height of dam			0.36	0.36
	...	0.24	0.24	0.36
Thickness of dam			0.09	0.09
	...	0.09	0.09	0.09
Size of the hole in the second dam	...	...	...	0.12× 0.085

(a) Weir/dam. (b) Dam/weir/dam. (c) Dam/weir/two dams (one containing a hole).

Table 3 Data of the Tundish Dimensions and Operation Conditions Used in the Calculations

Half length of tundish, m	3.37
Density of water, kg/m^3	1000
Viscosity of water, kg/m · sec	0.001
Density of inclusion, kg/m^3	920
Size of inlet nozzle, m^2	0.0081
Size of outlet nozzle, m^2	0.0081
Inlet velocity, m/sec	1.365
Outlet velocity, m/sec	1.365
Initial liquid level, m	0.9

4. Numerical Procedures

4.1 *Mathematical Model System Description*

Only one half of the modeled tundish was considered in the computations due to its axial symmetry. Figure 3 shows the modeled tundish with dotted lines and their dimensions. The numerical scheme of SOLA-SURF in conjunction with the K-ε turbulence model, used in this study, is the explicit finite difference method with regular meshes. A staggered grid system, in which velocity components are stored midway between the scalar (P, K, and ε) storage locations, was used. Then, governing equations were transformed to their finite difference forms.

4.2 *Solution Algorithm*

Here, the velocity field, particle path lines, and residence time distribution curves with respect to the steady-state flow field were the primary concerns. To obtain the velocity field, the following steps were taken to complete one calculational cycle:

- Identify the flow domain, for which the velocity field, K, ε, and ν_e are to be calculated, based on the height function distribution.
- Calculate the new tentative velocities for the entire fluid domain based on the finite difference form of the momentum equations with the velocity and pressure values ob-

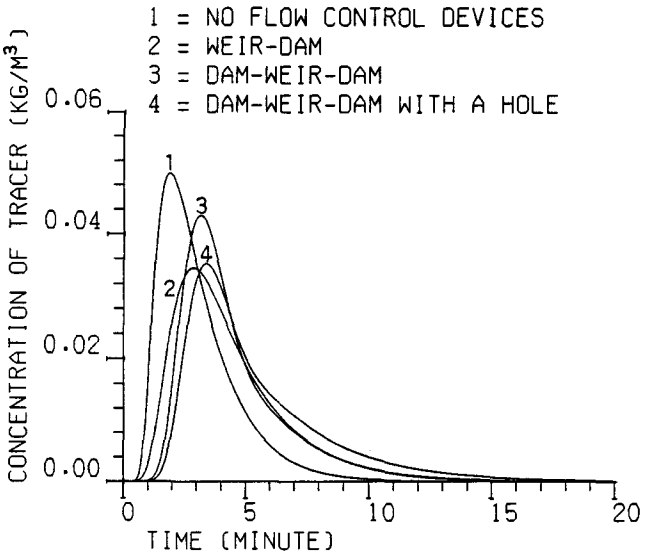

Fig. 4 Residence time distribution curves for tundishes incorporating various combinations of flow control devices.

Table 4 Data Obtained from the Residence Time Distribution Curves

Parameter data	Test case 1	2	3	4
Physical model				
t_{min}, sec	38	56	85	102
t_{mean}, min	5.22	5.66	5.84	6.00
Mathematical model				
t_{min}, sec	31	39	64	72
t_{peak}, min	1.89	2.86	2.96	3.40
t_{mean}, min	2.84	4.03	4.18	4.96

Note: See text for configuration used in test cases.

tained in the previous calculational cycle or prescribed earlier.

- Adjust these velocities iteratively to satisfy the continuity equation. In the iterations, each cell is considered successively and is given a pressure adjustment term that gradually drives its instantaneous velocity divergence to zero.
- As convergence is achieved, modify the height of the fluid surface. When the steady-state problem is considered, the calculations are repeated until the velocity field converges.

When the steady-state flow field was obtained, the particle path lines were calculated with Eq 9 to 11, and the variation of concentration with Eq 12 to obtain the residence time distribution curve.

5. Results and Discussion

Because the internal configuration of the tundish affects the flow field, favorable flow conditions for the removal of nonmetallic inclusions can be achieved by properly inserting flow

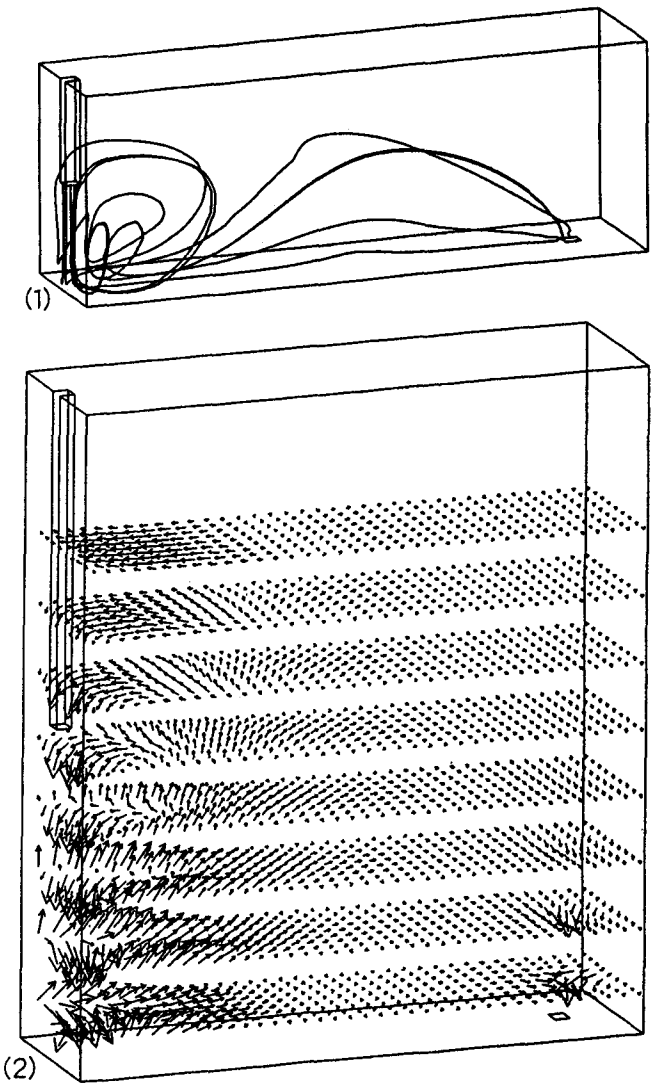

Fig. 5 Isoparametric view of the calculated particle path lines in the tundish with no flow control devices (1). Isoparametric view of the calculated three-dimensional flow field in the tundish with no flow control devices (2).

control devices in the tundishes. To demonstrate how the model can be used to gain better insight to the flow behavior of molten steel in tundishes of various designs, several cases were analyzed by the model developed in this study. However, before the model can be used to evaluate the different designs, it has to be verified for its accuracy and reliability. Because the system configuration considered in the mathematical model is slightly different from that of the physical model, as described in Section 2.1 and Fig. 1, verification cannot be done on an absolute-value basis. Rather, verification was done by comparing the semiquantitative trend.

Because most of the data obtained from the physical model consist of the residence time distribution curves and the characteristic parameters obtained from these curves, such as t_{min}, t_{peak}, and t_{mean}, the mathematical model was first used to calculate the residence time distribution curves and their corre-

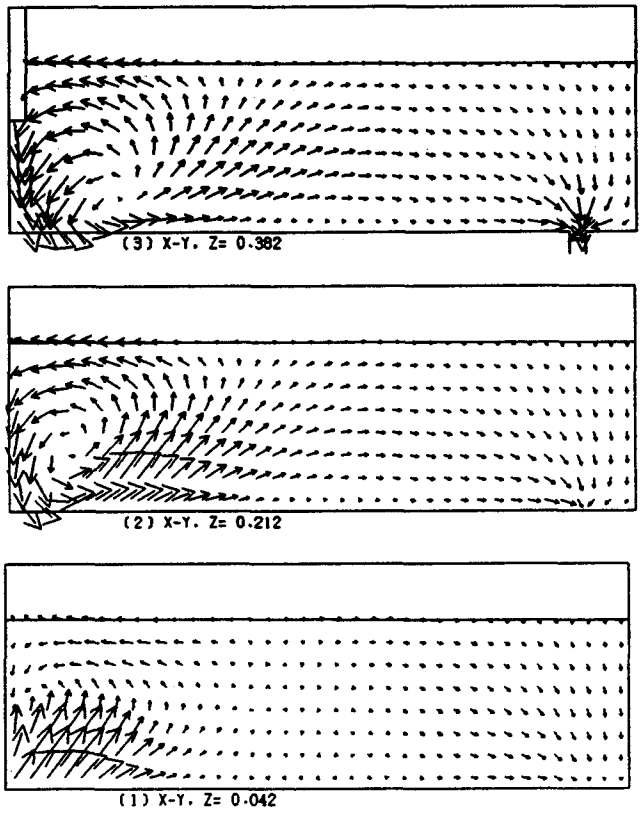

Fig. 6 Two-dimensional view of the calculated velocity profiles in the x-y planes for various z-coordinates in the tundish with no flow control devices.

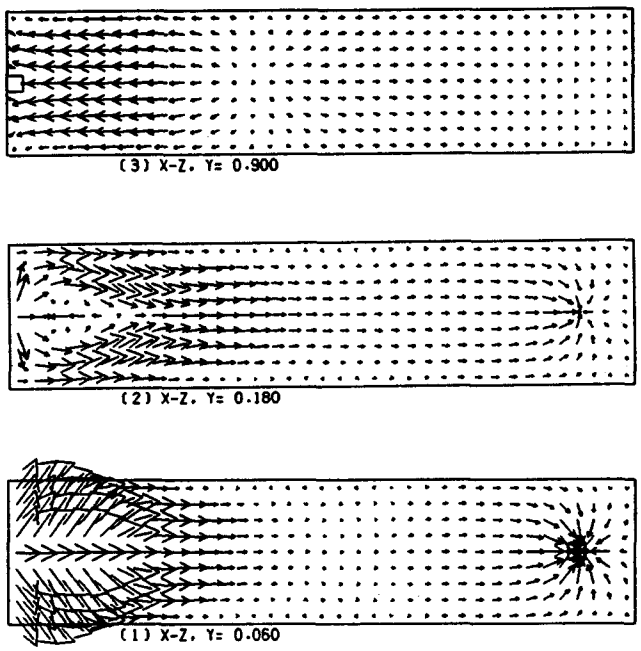

Fig. 7 Two-dimensional view of the calculated velocity profiles in the x-z planes for various y-coordinates in the tundish with no flow control devices.

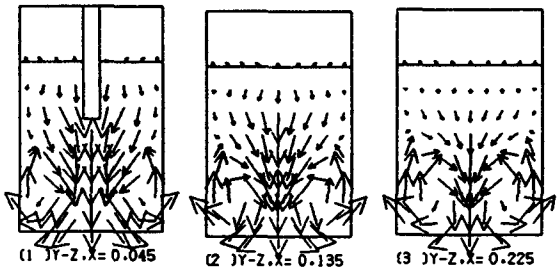

Fig. 8 Two-dimensional view of the calculated velocity profiles in the y-z planes for various x-coordinates in the tundish with no flow control devices.

sponding parameters. Also, because semiquantitative trend are being compared, a number of different tundish designs would have to be calculated by the mathematical model. System parameters for these various designs are shown in Table 2. Tundish dimensions and operation data used for the calculations are shown in Table 3. The simulated liquid used to compare with the experimental data of the physical model was water. The system was divided into 37 by 10 by 9 cells for X (longitudinal), Y (vertical), and Z (transverse) directions, respectively. The locations of the inlet and outlet nozzles are shown in Fig. 3. The positions of the flow control devices in the mathematical model were the same as the water model.

To study the steady-state operation, the inlet velocity was equal to the outlet velocity. As the steady-state velocity field is obtained, the transport of tracers is calculated based on the mass transport equation (Eq 12) and then the residence time distribution curves can be plotted. The residence time distribution curves calculated for the various designs listed in Table 2 are shown in Fig. 4. The horizontal and vertical axes of the residence time distribution curves are time and the concentration of the tracer, respectively. The curves show the variation in concentration with respect to time. From these curves, t_{min} and t_{peak} can be derived, and t_{mean} can be calculated based on Eq 14. These residence times are shown in Table 4. The residence time data obtained for four different designs from the physical model are also shown in Table 4. As the data of the physical model and those of the mathematical model are compared, the trend of the variation of t_{min} and t_{mean} obtained from the mathematical model is similar to that obtained from the water model. It demonstrates that the mathematical model is rather accurate and reliable, at least when the semiquantitative trend of the flow behavior in the tundishes of different designs is considered.

Now that the mathematical model has been verified, it is then ready to evaluate the effects of various designs. The calculated results for various cases will be discussed in the following sections. To understand the flow behaviors of the inclusion particles and to evaluate the effect of the flow control devices on the efficiency of inclusion removal, five particles (10 μm in size) were released from the inlet nozzle. The particle path line simulates how the inclusions flow along with the molten steel.

It is worth mentioning that the mathematical model developed in this study is currently implemented in an IBM personal computer. A typical run requires about 45 hr for the computa-

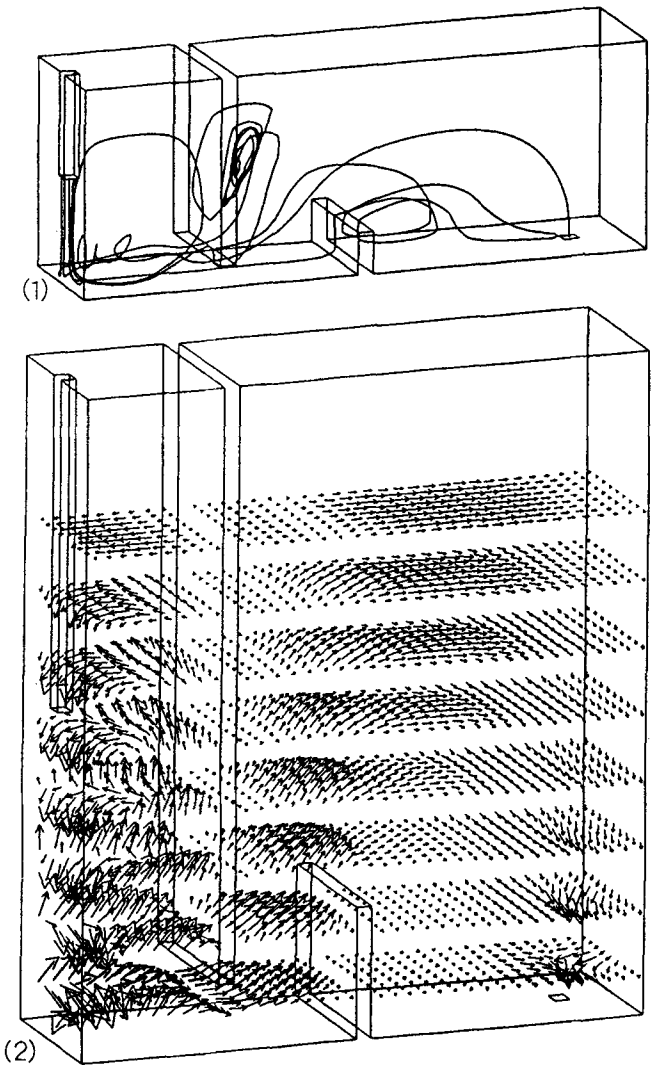

Fig. 9 Isoparametric view of the calculated particle path lines in the tundish incorporating a weir and a dam (1). Isoparametric view of the calculated three-dimensional flow field in the tundish with a weir and a dam (2).

tion of flow field and tracer dispersion on an IBM-PC386 with a 80387 coprocessor, and the calculation of particle path lines requires an additional 10 to 20 min. To demonstrate the calculated results, three sets of figures were plotted—first the isoparametric view of the particles path lines, second the isoparametric view of the three-dimensional velocity field with velocity vectors, and third the various two-dimensional sectional views of the velocity field.

5.1 *Case History 1: Tundish Without Flow Control Devices*

The first case to be reviewed is a tundish with no flow control devices. The computed velocity field and inclusion path lines are presented in Fig. 5 to 8. Figure 5 (part 1) shows the three-dimensional particle path lines, and Fig. 5 (part 2) shows the three-dimensional flow field in the tundish. To clearly illustrate the flow field, the scale of the *y* axis was mag-

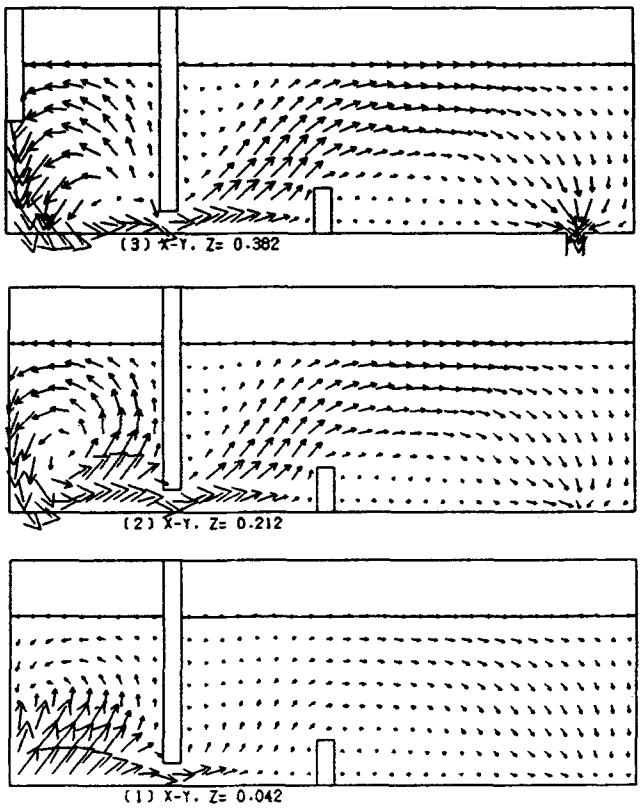

Fig. 10 Two-dimensional view of the calculated velocity profiles in the *x-y* planes for various *z*-coordinates in the tundish with a weir and a dam.

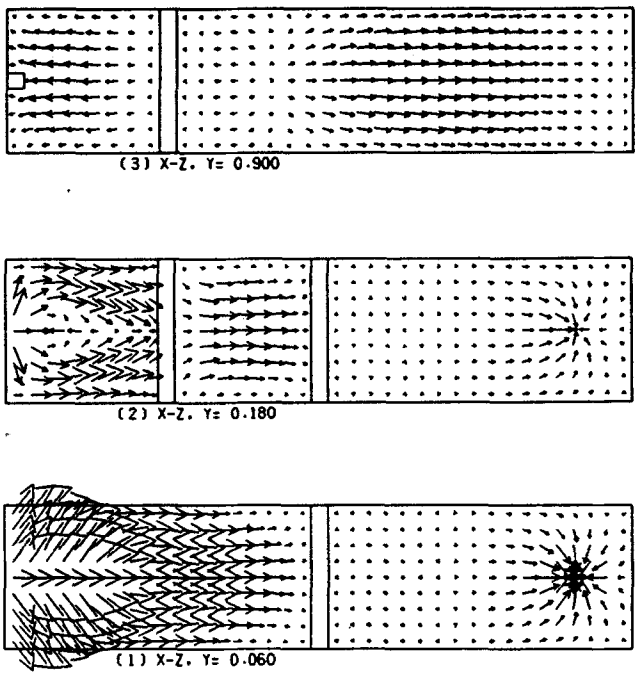

Fig. 11 Two-dimensional view of the calculated velocity profiles in the *x-z* planes for various *y*-coordinates in the tundish with a weir and a dam.

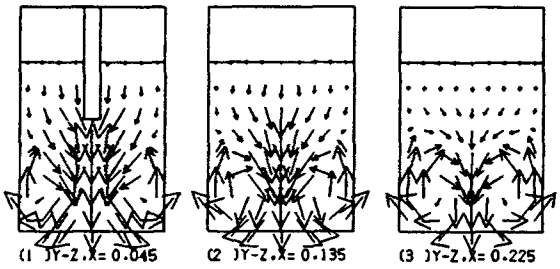

Fig. 12 Two-dimensional view of the calculated velocity profiles in the y-z planes for various x-coordinates in the tundish with a weir and a dam.

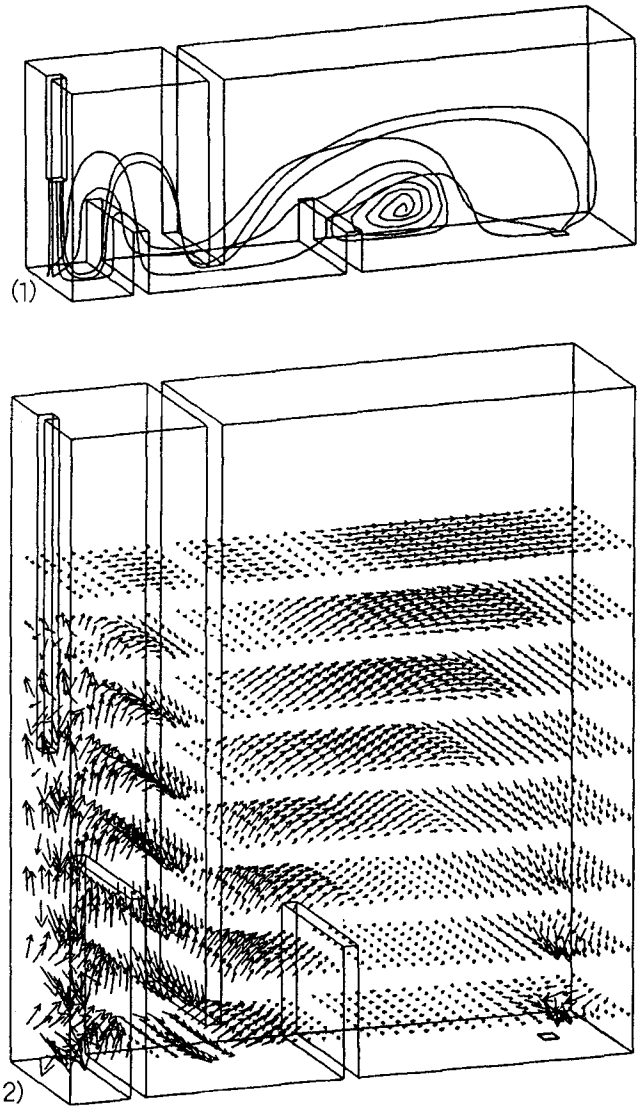

Fig. 13 Isoparametric view of the calculated particle path lines in the tundish with a weir and two dams (1). Isoparametric view of the calculated three-dimensional flow field in the tundish with a weir and two dams (2).

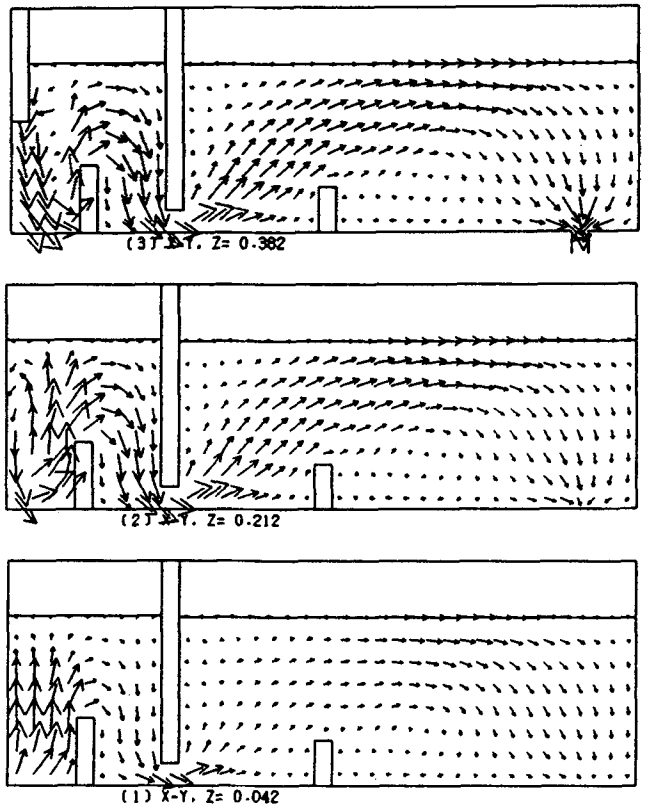

Fig. 14 Two-dimensional view of the calculated velocity profiles in the x-y planes for various z-coordinates in the tundish with a weir and two dams.

nified in Fig. 5 (part 2). Figure 6 shows the two-dimensional view of the calculated velocity profiles in the x-y planes for various z coordinates. The front wall corresponds to $z = 0$. Figure 6 (part 3) represents the velocity profile in the sectional plane through the incoming jet and exit nozzle, and Fig. 6 (part 1) shows the flow near the wall. Figure 7 illustrates the two-dimensional view of the calculated velocity profiles in the x-z planes for various y coordinates. The bottom wall corresponds to $y = 0$. Figure 8 shows the two-dimensional view of the calculated velocity profiles in the y-z planes for various x coordinates. The central plane corresponds to $x = 0$.

As Fig. 5 (part 2) and 6 (part 3) show, the entering stream flows down to the bottom and spreads radially, as shown in Fig. 7 (part 1). Figures 5 (part 2), 6, and 8 (parts 1 and 3) demonstrate strong recirculation near the inlet nozzle. The entering jet entrains liquid from its surroundings, causing a reverse flow near the area that is about one third of the total tundish length away from the inlet nozzle, as shown in Fig. 7 (part 3) and an upward flow near the front and rear walls, as shown in Fig. 6 (part 1). The forward flow near the bottom and the backward flow near the free surface cause a very large area of recirculation, as shown in Fig. 6 (parts 2 and 3). The fluid flows toward the exit nozzle, primarily near the level that is about one third of the total tundish height (see Fig. 5 (part 2) and 7 (part 2)). This suggests that nonmetallic inclusions may not have an opportunity to float up and become trapped by the surface slag. As shown in Fig. 5 (part 1), the path lines of the inclusions show lit-

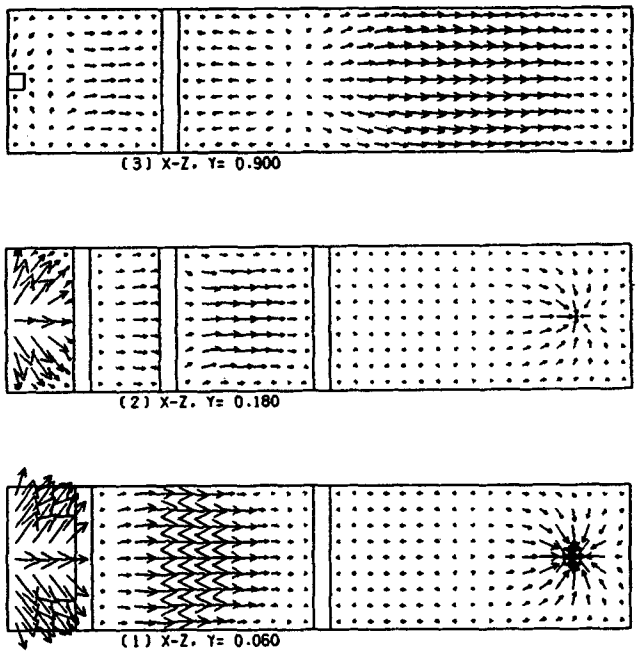

Fig. 15 Two-dimensional view of the calculated velocity profiles in the x-z planes for various y-coordinates in the tundish with a weir and two dams.

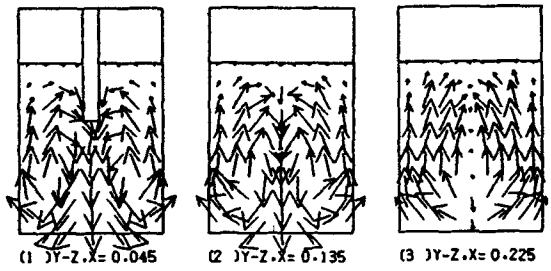

Fig. 16 Two-dimensional view of the calculated velocity profiles in the y-z planes for various x-coordinates in the tundish with a weir and two dams.

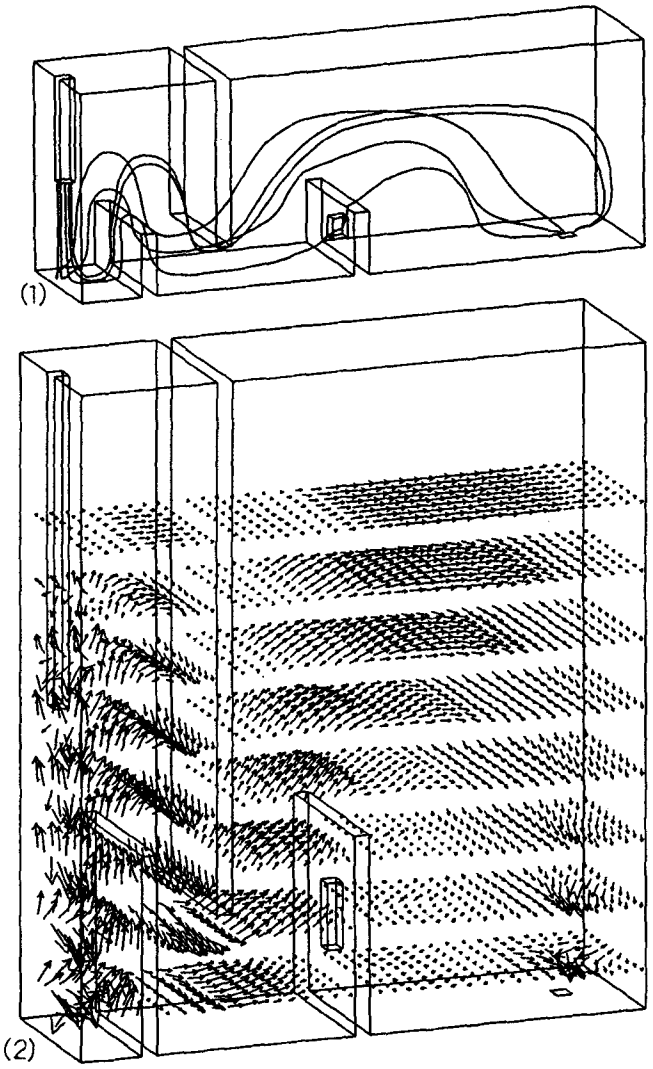

Fig. 17 Isoparametric view of the calculated particle path lines in the tundish with a weir and two dams (one of the dams contains a hole) (1). Isoparametric view of the calculated three-dimensional flow field in the tundish with a weir and two dams (one of the dams contains a hole) (2).

tle chance for the particles to make contact with the slag and to become absorbed by the surface slag. Additional supporting evidence is given in Table 4, where t_{min} for this case is rather small and t_{min} is believed to be closely related to the short-circuiting of fluid flow in tundishes. Figure 7 (part 1) illustrates sink-like vortex behavior near the exit nozzle.

5.2 *Case History 2: Tundish with a Weir and a Dam*

In this case, both a weir and a dam were added in the tundish. The particle path lines and computed flow field are shown in Fig. 9 to 12. The figures show that an area of strong recirculation develops between the inlet and the weir, and two weak ones appear on the back of the weir and the dam, respectively. The liquid is forced under the weir and then forced to flow upward above the dam. The fluid flows predominantly near the free surface and proceeds toward the end wall and then reflects and flows toward the exit, as shown in Fig. 9 (part 2), 10, and 11 (part 3). The various residence times for this case are longer than those of Case 1, shown in Table 4.

5.3 *Case History 3: Tundish with a Weir and Two Dams*

In this case, the flow field and particle path lines in the tundish with one weir and two dams were studied. The dam near the inlet nozzle forms a pool to reduce the erosion on the tundish bottom. The computed results are presented in Fig. 13 to 16. The dams force the fluid to proceed upward. The weir behind the first dam lengthens the flow paths of the liquid and the particles. From Fig. 13 (part 1), one particle is found to rotate behind the second dam where a dead zone has developed.

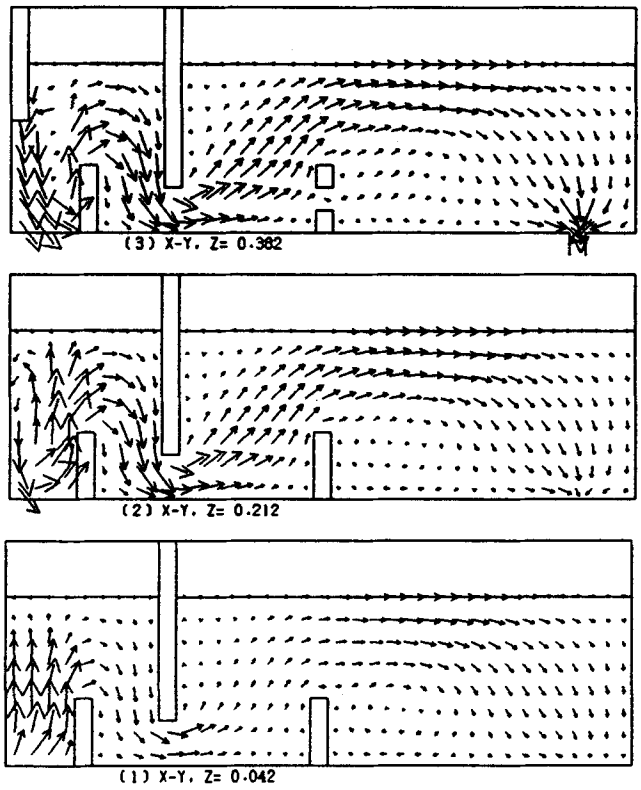

Fig. 18 Two-dimensional view of the calculated velocity profiles in the x-y planes for various z-coordinates in the tundish with a weir and two dams (one of the dams contains a hole).

5.4 *Case History 4: Tundish with a Weir and Two Dams (One Dam Contains a Hole)*

Although dams can improve the flotation of particles and reduce the erosion on the weir, as shown in Case 3, the amount of residual steel is considerable at the completion of the casting operation. To reduce the residual steel and alleviate the extent of the dead zone behind the dam, a hole was drilled in the second dam. The flow field thus calculated is illustrated in Fig. 17 (part 2) and 18 to 20. The particle path lines are shown in Fig. 17 (part 1). The first dam forces the fluid to proceed upward, the weir behind the first dam lengthens the flow path of the liquid, and the second dam containing a hole not only forces the fluid to proceed upward, but reduces the amount of residual steel at the end of the casting operation. It is interesting to note that the direction of fluid flow is slightly upward behind the second dam, as shown in Fig. 18 (part 3). Therefore, the particles will not flow directly to the exit. This is also evident in Fig. 17 (part 1).

5.5 *Residence Time Distribution Curves and Residence Times for Tundishes*

The residence time distribution curves and the resulting residence times are shown in Fig. 4 and Table 4, respectively. From Fig. 4, it can be seen that the curve of Case 1 rises first and, therefore, has the shortest t_{min} of all the other cases, as confirmed by Table 4. The same phenomenon is also demonstrated

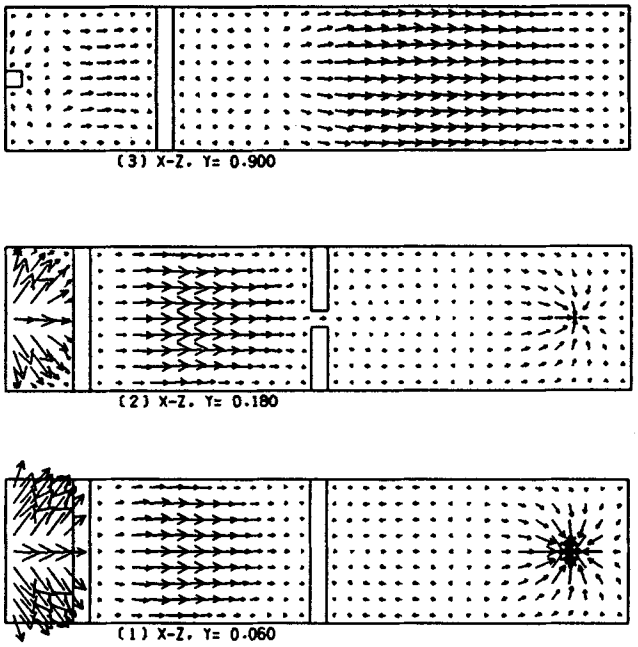

Fig. 19 Two-dimensional view of the calculated velocity profiles in the x-z planes for various y-coordinates in the tundish with a weir and two dams (one of the dams contains a hole).

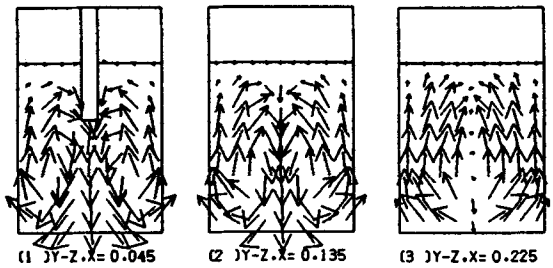

Fig. 20 Two-dimensional view of the calculated velocity profiles in the y-z planes for various x-coordinates in the tundish with a weir and two dams (one of the dams contains a hole).

by the t_{peak} and t_{mean} curves. Therefore, the design of Case 1 is unfavorable.

The curves of Cases 3 and 4 shift to the right in Fig. 4 and have longer residence times than all the other cases, which is also evident in Table 4. Therefore, these are the more favorable tundish designs. Moreover, the second dam containing a hole in Case 4 reduces the amount of residual steel and does not shorten the residence time and thus can be considered the most favorable tundish design.

6. Conclusions

In this study, a three-dimensional mathematical model was developed, based on the incorporation of a computational fluid dynamics technique, called SOLA-SURF, and the K-ε turbulence model. The mathematical model was first verified by comparing it to a full-scale water/plexiglas model. The charac-

teristics of the flow phenomena used in the comparisons were the semiquantitative trend of several characteristic parameters obtained from the residence time distribution curves. Because the model had been proven to be reasonably accurate and reliable, it was then used to analyze the flow behavior of the liquid and the nonmetallic inclusions in tundishes of various designs. The effects of the placement of various combinations of flow control devices (such as weirs, dams, and a dam containing a hole) on the efficiency of nonmetallic inclusion removal were then evaluated. The evaluation was based on the various residence times, such as t_{min}, t_{peak}, and t_{mean}, derived from the residence time distribution curves and path lines of the inclusions. A number of observations can be summarized as follows.

The three-dimensional turbulent flow behaviors of the liquid and the nonmetallic inclusion in the tundish can be observed in detail with the computed results of the mathematical model. The flow characteristics can be altered quite significantly by the use of various combinations of flow control devices.

The design incorporating the use of a weir tends to suppress the flow at the bottom of the tundish. However, the presence of the weir can restrain the flow turbulence introduced by the high-velocity liquid stream impinging from the ladle nozzle. Using a dam tends to stop the fast moving liquid near the bottom and force the liquid to proceed upward and over the dam. This prolongs the residence time and provides better path lines for removal of the inclusions. Therefore, the design using a combination of a weir/dam offers the best advantages of both components. It is thus a recommended design.

The design using a dam/weir/dam causes similar effects to that of a weir/dam. However, the residence time is longer, and particle path lines are even more favorable. If ultraclean steel is to be produced, this design is recommended. The second dam containing a hole does not produce any significant changes to the flow patterns while reducing the residual steel at the end of the casting.

Tests of the three-dimensional mathematical model demonstrate that the model can provide a great deal of useful information leading to a better understanding of the flow behavior of the liquid and nonmetallic inclusions in tundishes under various design conditions. It is also very flexible. The design and operating conditions can be changed quite easily, and the effects of the changes on the outcome can be evaluated readily. With the aid of this design tool, tundish design can be accomplished in a more systematic and scientific way to produce cleaner continuously cast steel.

Acknowledgment

The authors are grateful for the financial support for this study from China Steel Corporation under Project TRC-77-43.

References

1. Y. Sahai and R. Ahuja, *Ironmaking and Steelmaking*, *13*(5), 241-247 (1986).
2. T. DebRoy and J.A. Sychterz, *Metall. Trans. B*, *16*, 497-504 (1985).
3. J. Szekely and N. El-Kaddah, *Steelmaking Proceedings*, ISS-AIME, *69*, 761-776 (1986).
4. K.H. Tacke and J.C. Ludwig, *Steel Res.*, *58*, 262-270 (1987).
5. K.Y.M. Lai, M. Salcudean, S. Tanaka, and R.I.L. Guthrie, *Metall. Trans. B*, *17*, 449-459 (1986).
6. Y. He and Y. Sahai, *Metall. Trans. B*, *18*, 81-92 (1987).
7. J.L. Yeh, H.J. Lin, C.L. Chou, and W.S. Hwang, *J. Mater. Eng.*, *12*(2), 167-175 (1990).
8. C.W. Hirt, B.D. Nichols, and N.C. Romero, Los Alamos Scientific Laboratory Report LA-5852 (1975).
9. B.E. Launder and D.B. Spalding, *Mathematical Models of Turbulence*, Academic Press, New York (1972).
10. B.E. Launder and D.B. Spalding, *Computer Methods in Applied Mechanics and Engineering*, Vol 3, 269-289 (1974).
11. B.D. Nichols and C.W. Hirt, *J. Computational Phys.*, *8*, 434-448 (1971).
12. J. Szekely, *Fluid Flow Phenomena in Metals Processing*, Academic Press, New York (1979).